

Calculated Coupling Efficiency Between an Elliptical-Core Optical Fiber and a Silicon Oxynitride Rib Waveguide

Margaret L. Tuma and Glenn Beheim
(*Lewis Research Center*)
(*Cleveland, Ohio*)

Corrected Copy

Prepared for the
1995 International Symposium on Lasers and Applications
sponsored by the Society of Photo-Optical Instrumentation Engineers
San Jose, California, February 4–10, 1995



National Aeronautics and
Space Administration

(NASA-TM-106850) CALCULATED
COUPLING EFFICIENCY BETWEEN AN
ELLIPTICAL-CORE OPTICAL FIBER AND A
SILICON OXYNITRIDE RIB WAVEGUIDE
(NASA. Lewis Research Center) 15 p

N95-22915

Unclassified

G3/74 0042166

Calculated coupling efficiency between an elliptical-core optical fiber and a silicon oxynitride rib waveguide

Margaret L. Tuma and Glenn Beheim

NASA Lewis Research Center
Cleveland, OH 44135

ABSTRACT

The effective-index method and Marcatili's technique were utilized independently to calculate the electric field profile of a rib channel waveguide. Using the electric field profile calculated from each method, the theoretical coupling efficiency between a single-mode optical fiber and a rib waveguide was calculated using the overlap integral. Perfect alignment was assumed and the coupling efficiency calculated. The coupling efficiency calculation was then repeated for a range of transverse offsets.

Keywords: coupling efficiency, rib waveguide, elliptical fiber, effective-index, Marcatili's method

1. INTRODUCTION

The behavior of integrated-optic devices is often polarization sensitive. Polarization-preserving optical fibers can be used to couple light with a known polarization into these devices. In this study, the theoretical coupling efficiency between a polarization-maintaining elliptical-core fiber and a rib waveguide was investigated. To couple light energy efficiently from an optical fiber into a channel waveguide, the design of both components should provide for well-matched electric field profiles. Due to the complex geometry of a rib waveguide, there are no analytical solutions to the wave equation for the guided modes. Approximation techniques must be utilized to determine the propagation constants and field patterns of the guide. The two methods used here are the effective-index method¹⁻⁴ and Marcatili's approximation.⁵⁻⁷ The refractive index profile of the elliptical-core optical fiber was approximated by that of a rectangular channel guide,⁸⁻¹¹ for which an analytical solution can be determined.

There are several causes of coupling loss between a fiber and a waveguide.¹²⁻¹⁴ These include: transverse offset (x, y offset), mode field mismatch, longitudinal separation (z offset), tilt, and reflection. The loss mechanisms addressed in this study are the transverse offset and mode field mismatch. Mode field mismatch contributes significantly to interconnect loss,^{15,16} hence modeling is a necessary tool to design waveguides with low coupling loss. As misalignment in the x and y directions is inevitable in practice, the theoretical coupling efficiency results for x and y offsets are of interest.

The integrated-optic rib waveguide and elliptical-core optical fiber that are the subjects of this study are shown in Fig. 1. The single-mode channel waveguide is part of an integrated-optic

pressure sensor which is based on a strain sensitive ring resonator combined with a micromachined silicon diaphragm. This sensor can be interrogated with either quasi-TE or quasi-TM polarized light.¹⁷ In this investigation, only the TE mode was analyzed. A single-mode polarization-maintaining fiber with an elliptical core¹⁸ was used to excite the sensor at the 830 nm wavelength.

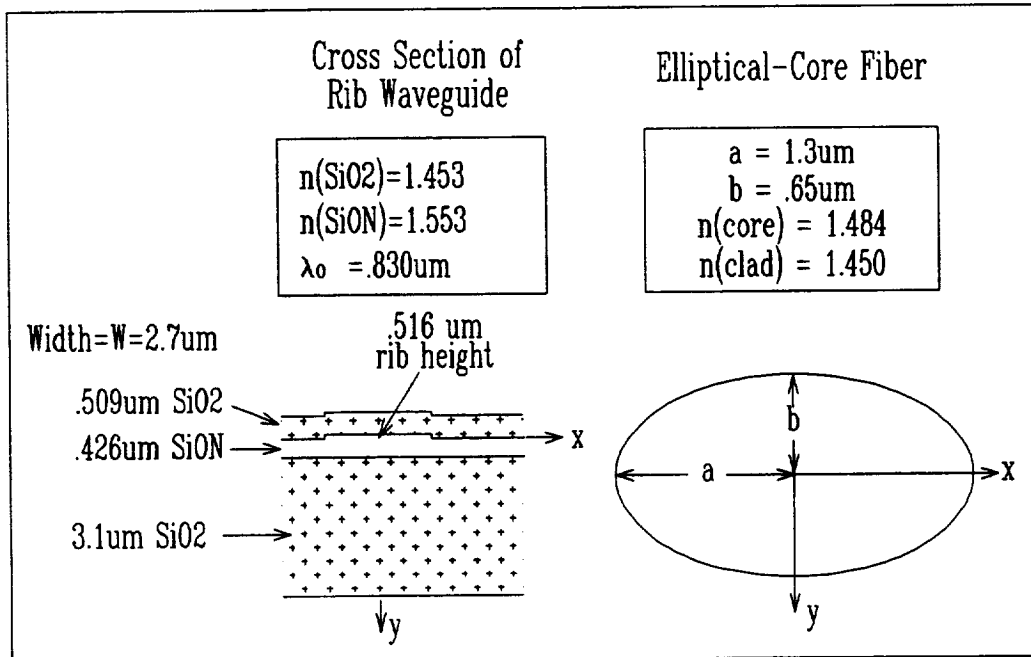


Figure 1: Rib channel waveguide and elliptical-core fiber.

2. RIB ELECTRIC FIELD CALCULATION - TWO TECHNIQUES

For the channel guide, two methods of calculating the propagation constant and electric field profiles were utilized: the effective-index method and Marcatili's technique. The TE modes are assumed excited and propagating in the z direction, thus the electric field is of the form

$$\vec{E}(x, y, z) = \hat{x} \Phi(x, y) e^{i(\omega t - \beta_o z)}, \quad (1)$$

where β_o is the propagation constant.

Both techniques provide solutions to the scalar wave equation,

$$\frac{\partial^2 \Phi(x, y)}{\partial x^2} + \frac{\partial^2 \Phi(x, y)}{\partial y^2} + [n^2(x, y) k_o^2 - \beta_o^2] \Phi(x, y) = 0. \quad (2)$$

In Eq. 2, $n(x, y)$ is the index of refraction and $k_o = \frac{2\pi}{\lambda_o}$, where λ_o is the wavelength in free space.

2.1 Effective-index method

The effective-index method reduces the two-dimensional scalar wave equation into two one-dimensional problems. First, the rib guide is divided into three separate planar guides oriented perpendicular to the y axis, as shown in Fig. 2. Slabs A and C, which have identical characteristics, correspond to the etched portion of the waveguide, while Slab B corresponds to the unetched portion. N_I is the effective index of Slab B and N_{II} is the effective index of Slabs A and C, where $N_{I,II} = \beta_{I,II}/k_0$. To determine the degree of confinement in the x direction, a symmetric slab waveguide, Slab D, is constructed which is perpendicular to the x axis. Slab D uses N_I and N_{II} as the core and cladding indices, respectively, and the rib width W as the core thickness. The analytic solution of Slab D yields the effective index, $N_{\text{effective}}$, of the rib guide.

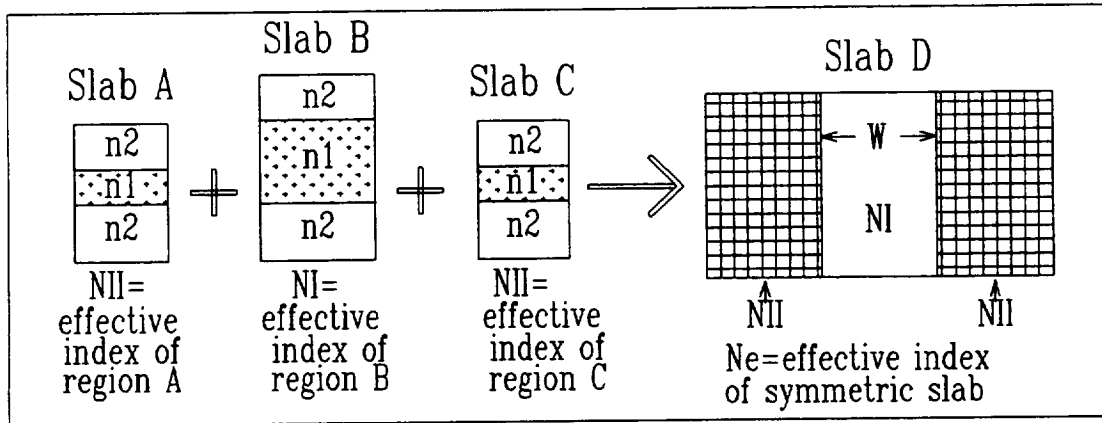


Figure 2: Effective-index method

The electric field profile of the rib is the product of the field distribution of Slab B, $X(x)$, and that of D, $Y(y)$, i.e.

$$\Phi(x, y) = X(x) Y(y). \quad (3)$$

The effective-index method has intuitive appeal. However, because the guide is analyzed as three separate slabs, the field continuity conditions at the interfaces are not met. The results of this method are most accurate for ribs with small height and large width.¹⁹ This condition is satisfied in this study as the guide etch depth is $.09 \mu\text{m}$ which is small when compared to its $2.7 \mu\text{m}$ width.

2.2 Marcatili's method

For modes far from cutoff, the majority of the field energy is confined in the central core region. For purposes of analysis, a pseudo-rectangular waveguide is utilized to approximate the

rib structure.¹¹ The cross section of the waveguide is divided into nine regions as shown in Fig. 3, in which t is the etch depth and r is the thickness of the etched silicon oxynitride (SiON) layer, such that the rib height is $r + t$.

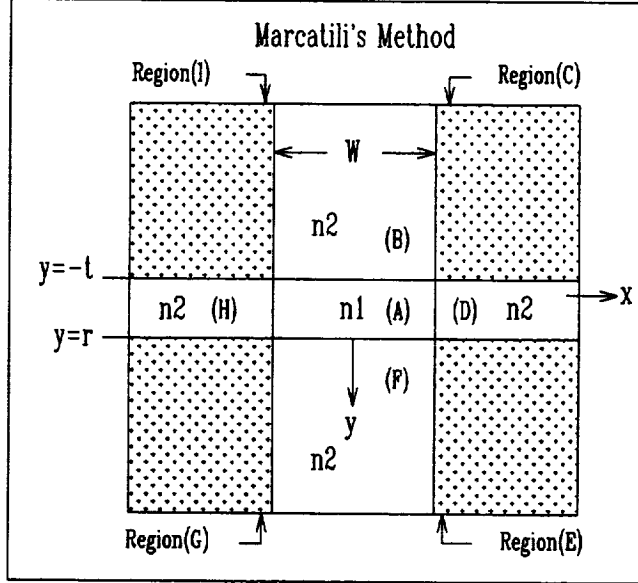


Figure 3: Marcatili's method: pseudo-guide used to approximate rib guide.

The pseudo-guide is assigned a refractive index profile which approximates that of the actual rib. This profile provides readier analysis because $n^2(x, y)$ is separable in the x and y coordinates; it is defined as¹¹

$$n^2(x, y) = n'^2(x) + n''^2(y) - n_1^2, \quad (4)$$

where

$$n'(x) = n_1 \quad \text{for } |x| < \frac{W}{2}, \quad (5)$$

$$n'(x) = n_2 \quad \text{for } |x| > \frac{W}{2}, \quad (6)$$

and

$$n''(y) = n_1 \quad \text{for } -t < y < r, \quad (7)$$

$$n''(y) = n_2 \quad \text{for } (y < -t) \text{ or } (y > r). \quad (8)$$

Analogous to the effective-index method, this method reduces the two-dimensional wave equation to two separate one-dimensional problems. Marcatili's technique is considered an approximate analytical approach and is most accurate when the waveguide mode is far from cutoff.⁵

Substituting Eqs. 3 and 4 into Eq. 2 produces

$$\left[\frac{d^2}{dx^2} + k_o^2 n'^2(x) - \beta_1^2 \right] X(x) = 0, \quad (9)$$

$$\left[\frac{d^2}{dy^2} + k_o^2 n''^2(y) - \beta_2^2 \right] Y(y) = 0, \quad (10)$$

where

$$\beta_1^2 + \beta_2^2 - k_o^2 n_1^2 = \beta_o^2. \quad (11)$$

When the mode is well-guided, the majority of the field energy is in the central core (n_1 region) which is a key assumption of this theory.⁵ The refractive index profile of the rib waveguide and pseudo-guide differ in the outer shaded regions and sections D and H of Fig. 3. The index of refraction in the shaded regions is $\sqrt{2n_2^2 - n_1^2}$. In regions D and H the actual index is n_2 when $-t < y < 0$ and n_1 when $0 < y < r$, but in this approximation it is assumed that n_2 is the index throughout regions D and H. However, because the modal power in these outer regions is small, the mode field profile of the pseudo-guide should closely resemble that of the rib guide. This assumption is generally applicable for large etch depths ($t \gg r$). However, for this channel guide the etch depth (t) is small, but because the rib is wide ($W \gg r + t$), it is expected that the pseudo-guide will provide an accurate field profile.

Following the development of Varshney and Kumar,¹¹ the x dependent solutions are

$$X(x) = A_1 \cos \left(2\mu_1 \frac{x}{W} - \theta \right) \quad \text{for } |x| < \frac{W}{2}, \quad (12)$$

$$X(x) = A_2 \exp \left(-2\mu_2 \frac{|x|}{W} \right) \quad \text{for } |x| > \frac{W}{2}, \quad (13)$$

where

$$\mu_1 = \frac{W}{2} \sqrt{k_o^2 n_1^2 - \beta_1^2}, \quad (14)$$

$$\mu_2 = \frac{W}{2} \sqrt{\beta_1^2 - k_o^2 n_2^2}, \quad (15)$$

and $\theta = 0$ ($\frac{\pi}{2}$) for a mode symmetric (antisymmetric) in x . The y dependent solutions are given by

$$Y(y) = A_b \exp \left(\frac{-\gamma_b y}{t} \right) \quad \text{for } y > r, \quad (16)$$

$$Y(y) = A_c \cos \left(\frac{\gamma_c y}{t} \right) + B_c \sin \left(\frac{\gamma_c y}{t} \right) \quad \text{for } -t < y < r, \quad (17)$$

$$Y(y) = A_a \exp \left(\frac{\gamma_a y}{t} \right) \quad \text{for } y < -t, \quad (18)$$

where

$$\gamma_b = t\sqrt{\beta_2^2 - k_o^2 n_2^2}, \quad (19)$$

$$\gamma_c = t\sqrt{k_o^2 n_1^2 - \beta_2^2}, \quad (20)$$

$$\gamma_a = \gamma_b. \quad (21)$$

Assuming quasi-TE polarized incident light, the boundary conditions,

$$n^2 \Phi(x, y) \text{ and } \frac{\partial \Phi(x, y)}{\partial x} \text{ continuous at } x = \pm \frac{W}{2}, \quad (22)$$

$$\Phi(x, y) \text{ and } \frac{\partial \Phi(x, y)}{\partial y} \text{ continuous at } y = -t, r, \quad (23)$$

are applied and eigenvalue equations determined for both the x and y dependent field functions. These eigenvalue equations are

$$\tan^{-1} \left[\frac{n_1^2 \mu_2}{n_2^2 \mu_1} \right] - \mu_1 + (p-1)\frac{\pi}{2} = 0, \quad (24)$$

$$\tan^{-1} \left[\frac{\gamma_a}{\gamma_c} \right] + \tan^{-1} \left[\frac{\gamma_b}{\gamma_c} \right] - \gamma_c \left(1 + \frac{r}{t} \right) + (q-1)\pi = 0, \quad (25)$$

for the x and y dependent field functions, respectively. For the fundamental mode, $p = q = 1$ in Eqs. 24 and 25. Constants A_1, A_2, A_a, A_b, A_c , and B_c are determined by satisfying the boundary conditions given in Eqs. 22 and 23.

3. FIBER ELECTRIC FIELD CALCULATION

The fiber in Fig. 1 was a single-mode polarization-maintaining elliptical-core fiber. Thus, the standard Gaussian approximation used for circular-core fibers is not valid for this case. Recently, several papers have discussed solutions for elliptical-core fibers.⁸⁻¹⁰ In this study, the elliptical core was approximated by a rectangle for which an analytical solution can be found. The rectangular core dimensions are chosen such that it and the elliptical core have the same area and aspect ratio.⁹ Therefore, the rectangle dimensions, a' and b' , are given by

$$a' = a \frac{\sqrt{\pi}}{2} \text{ and } b' = b \frac{\sqrt{\pi}}{2}. \quad (26)$$

A diagram of the elliptical and rectangular cores is shown in Fig. 4. Using this rectangle as the pseudo-guide, Marcatili's method (Section 2.2) was used to determine the fiber field profile. The field is given by Eqs. 12-21, where t and r have been replaced by b' , W has been replaced by $2a'$, and $B_c = 0$.

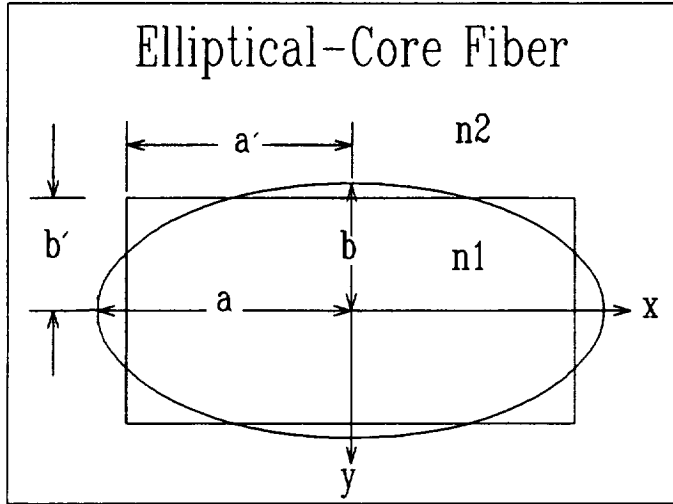


Figure 4: Elliptical-core fiber with pseudo-guide (rectangle).

4. COUPLING EFFICIENCY CALCULATION

Once the electric fields of the rib guide and fiber were calculated, the efficiency of coupling between the two components was determined. Because the index of refraction difference between the fiber and waveguide was small, Fresnel reflection loss was neglected.¹⁵ The coupling efficiency, η , was calculated using the overlap integral,^{14,17}

$$\eta = \frac{\left[\int \int \Phi_f(x, y) \Phi_g^*(x, y) dx dy \right]^2}{\left[\int \int \Phi_f(x, y) \Phi_f^*(x, y) dx dy \right] \left[\int \int \Phi_g(x, y) \Phi_g^*(x, y) dx dy \right]}, \quad (27)$$

where the integrals are taken over all space and $\Phi_f(x, y)$ and $\Phi_g(x, y)$ are the electric field profiles of the fiber and rib waveguide, respectively. The major axis of the elliptical-core fiber was oriented parallel to the x axis of the guide. The position of zero x and y offset is chosen to correspond to alignment of the maximum field positions of the fiber and rib.¹⁹ After solving for the aligned case, various x offsets were introduced and a new coupling efficiency calculated for each. This procedure was then repeated for various y offsets while the x offset was zero.

5. RESULTS

Field results for the elliptical fiber field using Marcatili's method are discussed in section 5.1. For the rib guide, the field profiles calculated using the effective-index method and Marcatili's approximation are described in section 5.2. The results of the theoretical coupling efficiency calculations for various x and y offsets are described in section 5.3.

5.1 Waveguide field results

Theoretical field results using the effective-index method and Marcatili's approximation are shown in Figs. 5 and 6. Results using the effective-index method tend to overestimate the width of the field in the x direction⁵ as illustrated in Fig. 5.

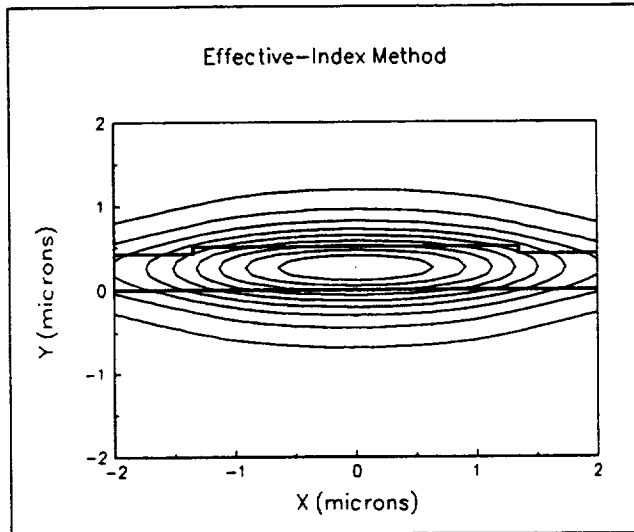


Figure 5: Effective-index method: electric field contours for rib guide.

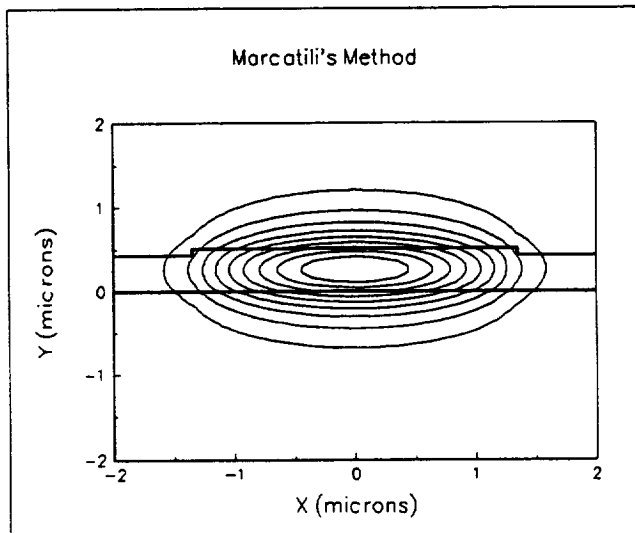


Figure 6: Marcatili's method: electric field contours for rib guide.

5.2 Fiber field results

Utilizing Marcatili's method, the fiber field profile was determined using the parameters $n_{core} = 1.484$ and $n_{clad} = 1.450$. The major and minor axes ($2a$ and $2b$) of the elliptical-core fiber were $2.6 \mu\text{m}$ and $1.3 \mu\text{m}$, respectively. A contour plot of the electric field is shown in Fig. 7. For all the contour plots in this paper, the contours indicate regions of equal field magnitude in increments of 0.1, with the maximum field magnitude being equal to 1.0.

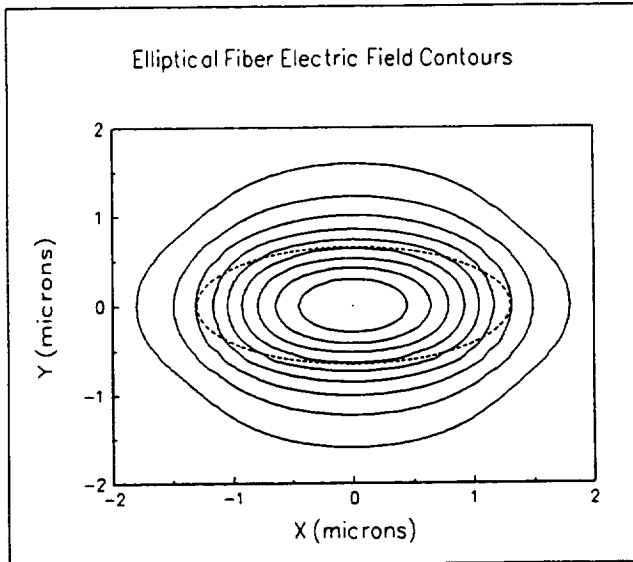


Figure 7: Fiber electric field contour plot with elliptical fiber core superimposed (dashed ellipse).

5.3 Coupling efficiency results

Once the alignment position was determined and the coupling efficiency at this position was calculated, an offset in the x direction was introduced. This offset ranged from $-3 \mu\text{m}$ to $+3 \mu\text{m}$ in $.20 \mu\text{m}$ increments. The coupling efficiency as a function of x offset is shown in Fig. 8.

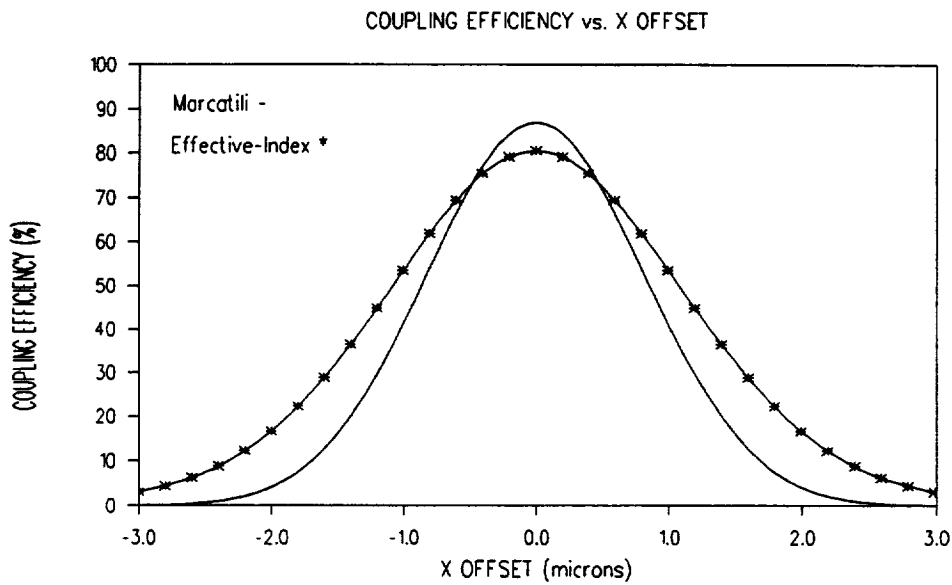


Figure 8: Coupling efficiency vs. *x* offset.

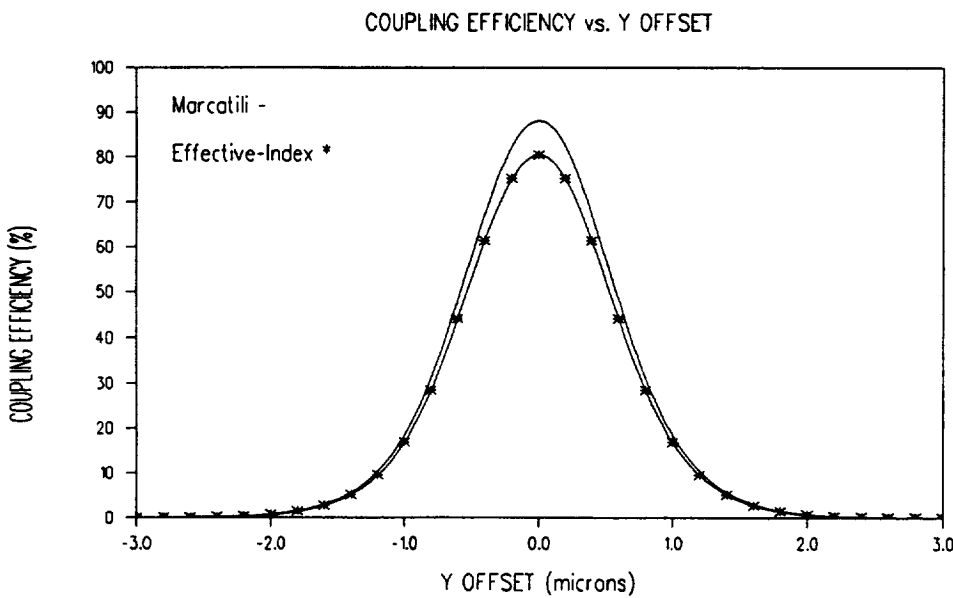


Figure 9: Coupling efficiency vs. *y* offset.

Similarly for the *y* direction, keeping the *x* alignment, the fiber position was varied from -3 μm to +3 μm from the position of alignment. The theoretical coupling efficiency results vs. *y* offset are shown in Fig. 9.

From the graphs in Figs. 8 and 9, it is apparent that alignment was more critical in the *y* direction. This is expected since the rib field calculated was more tightly confined in the *y*

direction than the lateral direction (x). The maximum theoretical coupling efficiency calculated was 81% using the effective-index method and 88% using Marcatili's technique. The actual coupling efficiency is expected to be somewhere between these two results. The difference was due to the weaker lateral rib field confinement predicted by the effective-index method, compared to the tighter confinement predicted by Marcatili's method. Because the fiber field profile more closely matches the rib field predicted by Marcatili's method, the theoretical coupling efficiency is higher than that calculated using the effective-index method.

6. CONCLUDING REMARKS

Theoretical coupling efficiency between an elliptical-core fiber and a rib guide was determined for a range of transverse offsets. Two techniques were used to calculate the theoretical electric field profile of the rib waveguide: the effective-index method and Marcatili's technique. For this channel structure, both methods produced similar results. The electric field profile of the elliptical-core fiber was determined using Marcatili's method.

Calculations of this kind are useful in optimizing the fiber choice and rib guide design in order to maximize the coupling efficiency between the two components.

7. ACKNOWLEDGMENTS

The authors wish to thank Helen Kourous and Greg De Brabander for helpful discussions regarding this work.

8. REFERENCES

1. R.M. Knox and P.P. Toulios, "Integrated circuits for the millimeter through optical frequency range," Proc. MRI Symposium on Submillimeter Waves, Polytechnic Press, Brooklyn, pp. 497-516, 1970.
2. Ramaswamy, "Strip-loaded film waveguide," Bell Syst. Tech. J., 53, pp. 697-705, 1974.
3. K.S. Chiang, "Review of numerical and approximate methods for the modal analysis of general optical dielectric waveguides," Opt. Quantum Electron., Vol. 26, pp. S113-S134, 1994.
4. G.B. Hocker, "Strip-loaded diffused optical waveguide," IEEE J. Quantum Electron., Vol QE-12, pp. 232-236, 1976.
5. D. Marcuse, Theory of Dielectric Optical Waveguides, pp. 330-334, 49-56, Academic Press, New York, 1991.
6. E.A.J. Marcatili, "Dielectric Rectangular Waveguide and Directional Coupler for Integrated Optics," Bell Syst. Tech. J., 48, pp. 2071-2102, 1969.
7. A. Kumar, K. Thyagarajan, and A.K. Ghatak, "Analysis of rectangular-core dielectric waveguides: an accurate perturbation approach," Opt. Lett., Vol. 8, No. 1, pp. 63-65, 1983.
8. A. Kumar and R.K. Varshney, "Propagation characteristics of dual-mode elliptical-core optical fibers," Opt. Lett., Vol. 14, No. 15, pp. 817-819, 1989.
9. A. Kumar and R.K. Varshney, "Propagation characteristics of highly elliptical core optical waveguides: a perturbation approach," Opt. and Quant. Electron., 16, pp. 349-354, 1984.
10. A. Kumar, R.K. Varshney, and K. Thyagarajan, "Birefringence calculations in elliptical-core optical fibers," Electron. Lett., Vol. 20, No. 3, pp. 112-113, 1984.
11. R.K. Varshney and A. Kumar, "A Simple and Accurate Modal Analysis of Strip-Loaded Optical Waveguides with Various Index Profiles," J. Lightwave Tech., Vol. 6, No. 4, pp. 601-606, 1988.
12. E.G. Neumann, Single-Mode Fibers, pp. 210-237, Springer-Verlag, Germany, 1988.
13. E.J. Murphy and T.C. Rice, "Self-Alignment Technique for Fiber Attachment to Guided Wave Devices," IEEE J. Quant. Electron., QE-22, No. 6, pp. 928-932, 1986.
14. R.G. Hunsperger, Integrated Optics: Theory and Technology, 2nd ed., p. 89, Springer- Verlag, New York, 1982.
15. Y. Cai, T. Mizumoto, E. Ikegami, and Y. Naito, "An Effective Method for Coupling Single-Mode Fiber to Thin-Film Waveguide," J. Lightwave Tech., Vol. 9, No. 5, pp. 577-583, 1991.
16. D.J. Vezzetti and M. Munowitz, "Design of Strip-Loaded Optical Waveguides for Low-Loss Coupling to Optical Fibers," J. Lightwave Tech., Vol. 10, No. 5, pp. 581-586, 1992.
17. G.N. De Brabander, J.T. Boyd, and G. Beheim, "Integrated Optical Ring Resonator with

Micromechanical Diaphragm for Pressure Sensing," IEEE Photonic Tech. Lett., Vol. 6, No. 5, pp. 671-673, 1994.

18. Andrew Corporation, D-series elliptical fiber, 205170-820F-2.
19. M.J. Robertson, S. Ritchie and P. Dayan, "Semiconductor waveguides: Analysis of coupling between rib waveguides and optical fibres," Integrated Optical Circuit Engineering II, SPIE, Vol. 578, pp. 184-191, 1985.
20. J. Albert and G.L. Yip, "Insertion loss reduction between single-mode fibers and diffused channel waveguides," Appl. Opt., Vol. 27, No. 23, pp. 4837-4843, 1988.

REPORT DOCUMENTATION PAGE

*Form Approved
OMB No. 0704-0188*

Public reporting burden for this collection of information is estimated to average 1 hour per response, including the time for reviewing instructions, searching existing data sources, gathering and maintaining the data needed, and completing and reviewing the collection of information. Send comments regarding this burden estimate or any other aspect of this collection of information, including suggestions for reducing this burden, to Washington Headquarters Services, Directorate for Information Operations and Reports, 1215 Jefferson Davis Highway, Suite 1204, Arlington, VA 22202-4302, and to the Office of Management and Budget, Paperwork Reduction Project (0704-0188), Washington, DC 20503.

1. AGENCY USE ONLY (Leave blank)			2. REPORT DATE January 1995		3. REPORT TYPE AND DATES COVERED Technical Memorandum		
4. TITLE AND SUBTITLE Calculated Coupling Efficiency Between an Elliptical-Core Optical Fiber and a Silicon Oxynitride Rib Waveguide			5. FUNDING NUMBERS WU-505-62-50				
6. AUTHOR(S) Margaret L. Tuma and Glenn Beheim							
7. PERFORMING ORGANIZATION NAME(S) AND ADDRESS(ES) National Aeronautics and Space Administration Lewis Research Center Cleveland, Ohio 44135-3191			8. PERFORMING ORGANIZATION REPORT NUMBER E-9438				
9. SPONSORING/MONITORING AGENCY NAME(S) AND ADDRESS(ES) National Aeronautics and Space Administration Washington, D.C. 20546-0001			10. SPONSORING/MONITORING AGENCY REPORT NUMBER NASA TM-106850 <i>Corrected copy</i>				
11. SUPPLEMENTARY NOTES Prepared for the 1995 International Symposium on Lasers and Applications sponsored by the Society of Photo-Optical Instrumentation Engineers, San Jose, California, February 4-10, 1995. Responsible person, Margaret L. Tuma, organization code 2540, (216) 433-8665.					12a. DISTRIBUTION/AVAILABILITY STATEMENT Unclassified - Unlimited Subject Categories 74 and 64		12b. DISTRIBUTION CODE
This publication is available from the NASA Center for Aerospace Information, (301) 621-0390.							
13. ABSTRACT (Maximum 200 words) The effective-index method and Marcatili's technique were utilized independently to calculate the electric field profile of a rib channel waveguide. Using the electric field profile calculated from each method, the theoretical coupling efficiency between a single-mode optical fiber and a rib waveguide was calculated using the overlap integral. Perfect alignment was assumed and the coupling efficiency calculated. The coupling efficiency calculation was then repeated for a range of transverse offsets.							
14. SUBJECT TERMS Coupling efficiency; Rib waveguide; Elliptical fiber; Effective-index; Marcatili's method					15. NUMBER OF PAGES 15		
					16. PRICE CODE A03		
17. SECURITY CLASSIFICATION OF REPORT Unclassified		18. SECURITY CLASSIFICATION OF THIS PAGE Unclassified		19. SECURITY CLASSIFICATION OF ABSTRACT Unclassified		20. LIMITATION OF ABSTRACT	